Visual Neuroscience (1991), 6, 197–206. Printed in the USA.

Nonlinearity of the inhibition underlying retinal directional selectivity

FRANKLIN R. AMTHOR[1] AND NORBERTO M. GRZYWACZ[2]

[1]Department of Psychology and Neurobiology Research Center, University of Alabama at Birmingham, Birmingham
[2]Center for Biological Information Processing, Massachusetts Institute of Technology, Cambridge, and The Smith-Kettlewell Eye Research Institute, San Francisco

(RECEIVED January 18, 1990; ACCEPTED August 20, 1990)

Abstract

An important mechanism for the discrimination of direction of motion in the retina is a spatially asymmetric inhibition. This inhibition has been postulated to operate either as a subtraction, like in difference-of-Gaussians models, or as a division, like in shunting-inhibition models of directional selectivity. The latter, but not the former, is nonlinear. This raises the question of whether the inhibitory mechanism involved in directional selectivity is nonlinear. To investigate this issue, we studied the linearity of the contrast dependence of the extracellularly recorded responses to apparent motions in ON-OFF directionally selective ganglion cells of the rabbit retina. The results show that the inhibition underlying directional selectivity is nonlinear and fits shunting-inhibition models well. Other biophysical mechanisms that might account for the type of nonlinearity observed in the data are also considered.

Keywords: Rabbit, Retina, Ganglion cells, Directional selectivity, Nonlinear inhibition, Shunting inhibition

Introduction

In the rabbit retina, an important mechanism for the selectivity of some ganglion cells to direction of motion is an asymmetric inhibitory process (Barlow & Levick, 1965; Wyatt & Daw, 1975). This asymmetry exists at every point in the receptive-field center, so that motions within small regions of the receptive-field center elicit directionally selective responses (Barlow & Levick, 1965). This process is apparently mediated by GABAergic inhibitory synapses (Caldwell et al., 1978; Ariel & Daw, 1982; Ariel & Adolph, 1985).

There are two main effects of inhibitory synapses: hyperpolarization and shunting (Coombs et al., 1955). Hyperpolarization tends to interact linearly with excitatory potentials (Jack et al., 1975; Grzywacz & Koch, 1987), by subtracting from the postsynaptic potential. Shunting tends to interact nonlinearly with excitation (Rall, 1964; Jack et al., 1975; Torre & Poggio, 1978), by dividing the voltage generated by excitatory synaptic currents via a reduction in postsynaptic resistance (Ohm's law). These two mechanisms are not mutually exclusive; hyperpolarizing synapses also have some degree of shunting-inhibition effects (Kandel & Schwartz, 1985).

Some models for retinal directional selectivity rely primarily on the shunting component of inhibition to explain the directional selectivity for short-motion stimuli (Torre & Poggio, 1978). In these models, pure shunting inhibition would lead to a better motion acuity than would hyperpolarizing inhibition because shunting inhibition could lead to local interactions between excitation and inhibition in the cells' dendrites (Torre & Poggio, 1978). Models of directional selectivity based on hyperpolarizing inhibition (Grzywacz & Koch, 1987) or purely linear inhibition (Adelson & Bergen, 1985; Heeger, 1987; Grzywacz & Yuille, 1990) have also been proposed. In these models, the linear inhibition mechanism mediates motion sensitivity by means of a temporal impulse response, which depends on the stimulus position within the receptive field. Strictly speaking, no purely linear mechanism can give rise to directional selectivity (Poggio & Reichardt, 1973). However, a linear inhibition can do so if followed by a half-wave rectification (Grzywacz & Koch, 1987). Such a rectification appears to be part of the cascade mediating the dynamics of certain ganglion cells (Shapley & Victor, 1980; Victor, 1987, 1988). Although this mechanism has the inherent danger that directional selectivity would be lost for high contrasts or bright backgrounds, the visual system might avoid this danger through the use of adaptational processes prior to the rectification.

Intracellular recordings have not revealed the inhibitory mechanism that underlies directional selectivity. Both hyperpolarizations in rabbits' directionally selective cells (Miller, 1979) and inhibited depolarizations (Amthor et al., 1989) have been reported. Resting-potential elevation following cell injury may result in apparent hyperpolarizations for pure shunting synapses. Studies with turtle (Marchiafava, 1979) and frog (Watanabe & Murakami, 1984) show shunting inhibition, but it is unclear if it is directly related to directional selectivity. For

Reprint requests to: Franklin R. Amthor, Department of Psychology, University of Alabama at Birmingham, Birmingham, AL 35294.

instance, the ganglionic inhibition might mediate gain control while a pre-ganglionic mechanism might underlie directional selectivity (Masland et al., 1984; Dowling, 1987; Vaney & Young, 1988; Devoe et al., 1989).

Because hyperpolarizing, but not shunting inhibition, tends to be linear, we decided to examine the linearity of the inhibition underlying directional selectivity. If the inhibitory synapse is linear but followed by a rectification, then even though the overall mechanism is nonlinear, it may be essentially linear for suprathreshold stimuli, as is the case for cortical simple cells (Albrecht & De Valois, 1981). The data described in this paper cannot rule out that an inhibitory synapse, which has a large hyperpolarizing effect and a small shunting-inhibition effect mediates the inhibition. What is actually tested is whether the inhibition is *linear in the mathematical sense*. This might sound strange, because even if a synapse could inject hyperpolarizing currents without changing membrane conductances, one would not expect it to be completely linear. For example, the synapse should saturate if its input is large. Nevertheless, the experiments presented here focused on the inhibitory effects elicited by small stimulus contrast ($\leq$30%). By doing so, we hoped to preserve the potential linearity of the synaptic mechanism.

We investigated the linearity of the inhibition by using two-slit apparent motions in the null direction (the direction eliciting the weakest cell responses). The responses of ON-OFF directionally selective ganglion cells to apparent motions, as to "real" continuous motions, are directionally selective (Barlow & Levick, 1965; Wyatt & Daw, 1975). For two-slit null-direction apparent motions, we determined the effect on the responses to the second slit of variation of the contrast of the first slit. Under the assumption of linear inhibition, the magnitude of this effect should be proportional to the first slit's contrast. Otherwise, if the inhibition is nonlinear, one can test the consistency of the emerging data with a division-like mechanism, and in particular, with shunting inhibition.

The responses we measured were the spikes recorded extracellularly from ON-OFF directionally selective ganglion cells of the rabbit retina. Extracellular recordings have two advantages: first, they allow the cells to be held for long periods of time, and second, they allow the action of the inhibitory mechanism to be studied regardless of whether it is pre- or postsynaptic to the ganglion cell. Holding the cell for long periods enables the characterization of the inhibitory interaction for a wide range of contrasts. The main disadvantage of extracellular recordings is that one can investigate the null-direction inhibitory mechanism only indirectly. For example, even if one finds a nonlinear mechanism, one cannot be sure that hyperpolarization does not mediate the main component of inhibition. The linear effect of hyperpolarization might be modified later in the process by a nonlinearity (see Discussion).

Methods

Preparation

Ten ON-OFF directionally selective ganglion cells of the rabbit retina were recorded extracellularly in an isolated eyecup preparation (Amthor et al., 1984, 1989). The eyes were from adult Dutch belt-pigmented rabbits (of both sexes) weighing at least 1.3 kg. All surgery was done in dim red light on animals which had been dark-adapted for at least 30 min. Animals were deeply anesthetized with an initial dose of urethane (2 g/kg), followed by Surital (Sodium Thiamylal, Fermenta Animal Health, Kansas City, MO) given to effect, that is, bringing the animal to a level of anesthesia in which no reflexive movement or change in heart rate resulted from a noxious stimulus, such as a pinch to the paw. After deep anesthesia was achieved, the right eye was enucleated as the animal was killed with a massive overdose of Surital. After enucleation the eye was briefly rinsed in ice-cold superfusate medium. The superfusate medium was similar to that described by Ames and Hastings (1956). The medium was equilibrated with 95% O_2 and 5% CO_2, and the pH was in the range of 7.35–7.45. The eyes were enucleated and hemisected behind the ora serrata, and the vitreous body lifted away. The remaining eyecup was placed in room-temperature superfusate and four radial cuts were made 2–3 mm inward from the margin of the retina to facilitate its subsequent eversion. The eyecup was then everted over an inflatable latex dome on a Teflon pillar that formed the bottom part of the superfusion chamber. The chamber was similar to that described by Dacheux et al. (1973). The superfusate was heated in a bath to 35.5–36.5°C and flowed over the retina at a rate of 3–7 ml/min.

Stimuli

The stimuli were generated by computer control of yellow light emitting diodes (slits). The slits were separated by a retinal distance ($\approx$30–90 μm) of about a fifth of the receptive-field size; preliminary experiments showed significant inhibitions for inter-slit distances more than half the receptive-field size (Grzywacz & Amthor, 1988). Intensity was square-wave modulated above and back to a background level, which was 25 $\mu W/cm^2$. Stimuli presentations were separated by 2–3 s interstimulus intervals to allow recovery to background adaptation state. Total responses were the spike-count means of from 18–60 trials. Each trial consisted in the presentation of the second slit in an ascending order of contrasts with the contrast of the first slit set to zero, and the same sequence repeated with increasing contrasts of the first slit (Fig. 1). The first slit onset and offset preceded the second slit onset and offset by 500 ms, respectively. At this delay, directionally selective inhibition was still strong (Amthor & Grzywacz, 1988), but few of the spikes due to the first slit fell in the second slit's data gathering window (500 ms after the second slit's onset and offset). The mean number of spikes, which occurred in this window, due to the first slit was subtracted from the window's responses.

Test of linearity

To test whether the apparent motion data indicate the inhibition is linear, we reasoned as follows. Let $R_0(t)$ be the time course of the suprathreshold response to the second slit presented in isolation. Next, let the suprathreshold response to the second slit when preceded by the first slit be $R_c(t)$, where c is the contrast of the first slit. We define the time course of the inhibitory strength to be

$$S_c(t) = R_0(t) - R_c(t). \quad (1)$$

Now consider the plot of $S_{c_2}(t)$ (at contrast c_2) as a function of $S_{c_1}(t)$ (at contrast c_1). If the inhibition is linear, this plot should be a straight line with zero intercept and with slope c_2/c_1. This is because under linear inhibition, there is a function $I(t)$ such that $R_c(t) = R_0(t) - cI(t)$. Thus, by directly substituting this expression for R_c into eqn. (1), one obtains that $S_c(t) = cI(t)$. Because $I(t)$ is common to all contrasts,

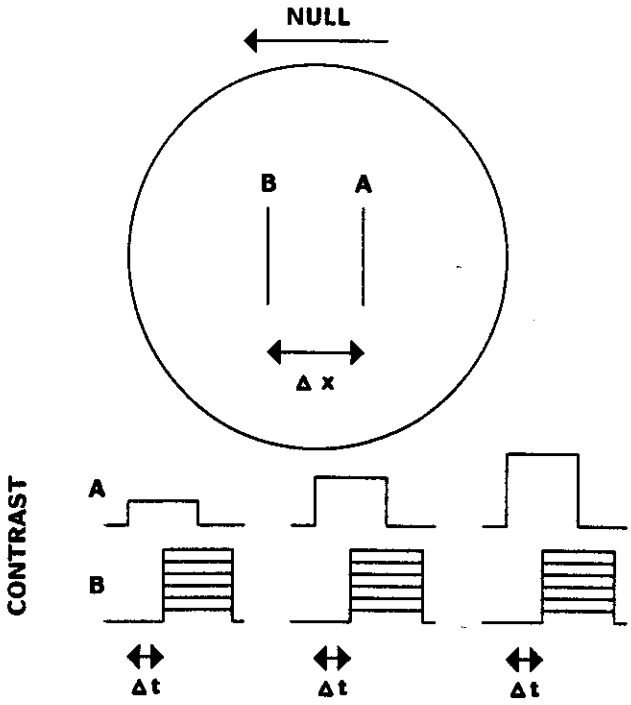

Fig. 1. Diagram of the visual display in the experimental protocol. We determined for apparent motion in the null direction the effect of varying the contrast of the first slit (A) on responses elicited by the second slit (B) also presented at various contrasts. Each trial consisted in the presentation of the second slit in an ascending order of contrasts with the contrast of the first slit set to zero, and the same sequence repeated with increasing contrasts of the first slit. The slits were on for 1 s and the delay between them, 500 ms, was generally longer than the duration of the first slit's response.

the $S_{c_2}(t)$ vs. S_{c_1} function should have the properties asserted above.

Thus, to test the inhibition's linearity, we first measured from poststimulus histograms (with 20 ms binwidth) the time course of the inhibitory strength parametric on the contrasts of the two slits. Then, pairs of inhibitory-strength time courses (generated with the same second slit contrast) were plotted against each other. These plots were added as linear sample regression lines. Also, statistical tests were made to determine whether the intercepts of the sample regression lines were zero, and whether their slopes were equal to the ratio between the first-slit contrasts (Dunn & Clark, 1987). To minimize threshold effects, we performed these calculations for those bins that satisfied two conditions for all contrasts of the first slit. First, a chosen bin and its two neighbors had to contain at least one spike each. Second, all of the bins between a chosen bin and the bin of maximal response had to have at least one spike. This analysis was performed for the ON and OFF responses separately.

Fitting procedure

To compare the data to the predictions of a division-like inhibitory mechanism, we proceeded as follows. A best least-squares nonlinear fit of the data to a shunting-inhibition model (see Results for model details) was calculated. The fit was made simultaneously to the mean of the suprathreshold integrated responses at all contrasts of the first and second slits. To perform the fit, we used a "quasi-Newton" convergence procedure (*Systat*, Systat Inc, Evanston, IL). This procedure has the advantage of a high speed of convergence if one starts with a sufficiently accurate initial approximation. In the present case, the simplicity of the model and the general appearance of the data immediately suggested good guesses for initial approximations. We used two different initial approximations for each data set to prevent the procedure from being trapped in local minima; this procedure will be disucssed in more detail after the introduction of the equations. The multiple correlation coefficient for the least squares nonlinear fit was calculated. This coefficient is calculated from the linear regression applied to the data-versus-fitted-model plot. Several recent statistical studies consider regression tests for arbitrary fits (for a review see Stephens, 1987).

Results

We determined for apparent motions in the null direction the effect of varying the contrast of the first slit on responses elicited by the second slit also presented at various contrasts (Fig. 1).

Figure 2 shows the mean poststimulus histograms of the responses of a cell to four apparent-motion stimuli presented over several trials. In these series of trials, the contrast of the second slit was 40% and the contrast of the first slit varied. Although the responses to the second slit (after B_{on} and B_{off}) is large when the first slit is absent, they markedly decrease when the first slit appears. Furthermore, their amplitude decreases as the first slit's contrast increases. Also, it is of significance that the first slit can precede the second slit by 500 ms and still generate inhibition. This result is due to the relatively sustained character of inhibition (Amthor & Grzywacz, 1988). The inhibition's response can last for more than 2 s during a maintained light stimulation (Amthor & Grzywacz, 1988). This long duration contrasts with the much shorter duration of excitation ($\approx$ 500 ms; Fig. 2).

Test of linear inhibition

Suppose, for the sake of argument, that the inhibition is linear and constant throughout the duration of the excitatory response. Then, the effect of the inhibition on the histograms of Fig. 2 should be to reduce the amplitude of all of the bins by the same amount. This is not what is observed in the histograms. Rather, the bins near the peak of the response are more affected than the bins with less spikes. An explanation for this difference is that the inhibition is nonlinear. For example, a division-like inhibition would affect more the higher portions of the response than the smaller ones. An alternative explanation is that the inhibition is linear, but that its maximal effect in time coincides with the peak of excitation. However, in other experiments, we found that the histograms appear to be relatively invariant for apparent-motion delays ranging from 100 ms to 2 s. This suggests that the time-course explanation is incorrect and that the inhibition might be nonlinear.

To develop this idea further, we tested whether the inhibition depends linearly on contrast throughout the time course of the excitation. Figure 3 shows a plot of the inhibitory strengths [eqn. (1)] obtained with the contrast of the first slit set to 20% *versus* the inhibitory strengths obtained with 10% contrast. Each data point represents inhibitory strengths measured at a fixed time bin. To minimize threshold effects, we used only those portions of the response that are suprathreshold (see

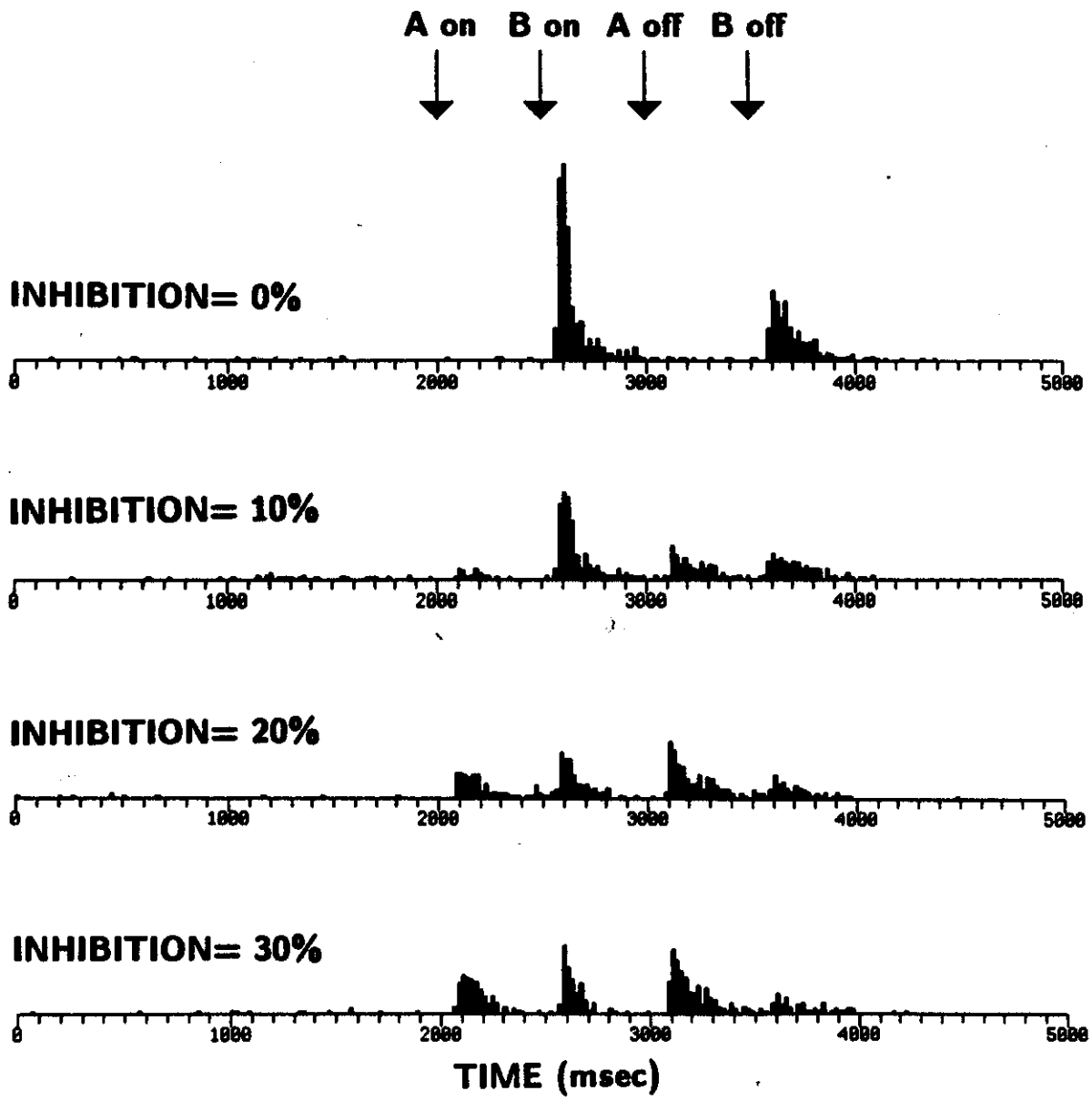

Fig. 2. Mean poststimulus histograms. This figure plots the histograms of the ON and OFF responses of cell E380.c31 to null-direction apparent motions. The contrast of the second slit is 40% and the contrast of the first slit (inhibition) varies. The amplitude of the responses to the second slit decreases as the contrast of the first slit increases. In addition to this inhibitory effect, the first slit produces excitatory ON and OFF responses. Also, it is of significance that the first slit can precede the second slit by 500 ms and still generate inhibition.

Methods). Also, Fig. 3 presents the ON–ON and the OFF–OFF sequences separately (Fig. 3A and 3B, respectively). As explained after eqn. (1), for a linear inhibition, this plot should (1) be a straight line, (2) have zero intercept, and (3) have a slope of 2 (the ratio between the contrasts of the first slit; that is, 20% over 10%). Conditions 1 and 2 are met in Fig. 3. The sample regression lines have high correlation coefficients (0.94 and 0.97 for the ON–ON and OFF sequences, respectively). Also, the intercepts of these lines are not significantly different than zero (two-sided *t*-test). However, one also sees in Fig. 3 that condition 3 is not met. The slopes of sample regression lines are smaller than 2 (1.26 for the ON–ON sequence and 1.06 for the OFF–OFF sequence). This discrepancy is statistically significant (two-sided *t-test*, $P < 0.001$ and $P < 0.0005$ for the ON–ON and OFF–OFF sequences, respectively). These statistical tests yielded similar results when performed on other contrasts of the second slit and on nine other cells. Thus, from the discrepancy between predicted and observed slopes of the sample regression line, we conclude that the inhibition is nonlinear.

From the test of linearity in Figure 3, one can learn about one more property of the inhibitory process: The inhibitory strength (eqn. (1)) is a separable function of contrast and time for low contrasts (≤30%). Because the inhibition is nonlinear, the assumption $S_c(t) = cI(t)$ is no longer valid. Hence, it becomes unclear how the inhibitory strength depends on both contrast and time. It is even unclear that the inhibitory strength is a separable function of these two variables, that is, that there is a function $J(c)$ such that $S_c(t) = J(c)I(t)$. However, this

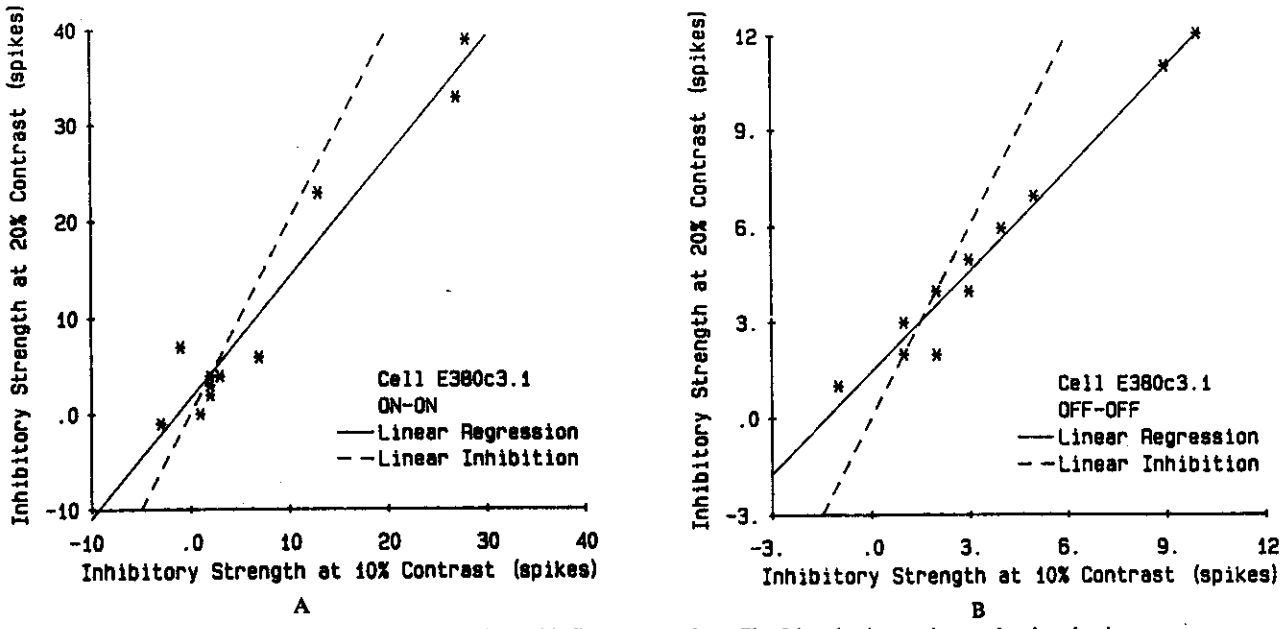

Fig. 3. A test of the linear-inhibition assumption. This figure comes from Fig. 2 by plotting against each other the time courses of the inhibitory strength [eq. (1)] for the 20% and 10% contrasts of the first slit. The axes' dimensions correspond to number of spikes in 20-ms bins. To minimize threshold effects, we used only those portions of the responses that are suprathreshold (see Methods). ON–ON and OFF–OFF sequences are shown in 3A and 3B, respectively. The figure also shows the sample regression lines (solid) and the lines predicted by the assumption of linear inhibition (dashed). The sample regression lines provide a good fit to the data and the intercepts of these lines are not significantly different than zero. However, the slopes of sample regression lines are smaller than expected by assuming linear inhibition, which indicates that the inhibition is nonlinear.

condition is necessary and sufficient for the data in Figure 3 to fall on a straight line. Therefore, since this is what happens, we conclude that the inhibitory strength is separable at low contrasts. Actually, the data only allow us to reach this conclusion for times near the maximum of the response. These are the times used in Figure 3 to avoid threshold effects (see Methods). In the Discussion, it will be argued that this separability property might not hold for later portions of the response.

What sort of nonlinearities can lead to the shallow slopes observed in Figure 3? In the Discussion, we will show that shunting inhibition can account for these slopes. Here, it will be briefly argued that a hyperpolarizing mechanism "spoiled" by an earlier nonlinearity can also explain the data presented so far. To see this argument, remember that the inhibitory strength is separable in contrast and time, that is $S_c(t) = J(c)I(t)$. It follows that the expected slope in the plot of Figure 3 is the ratio $J(c_2)/J(c_1)$. If $J(c)$ is a sublinear function, that is, its first derivative decreases with contrast, then the slope will be smaller than c_2/c_1 and larger than unity. This is similar to what is observed in Figure 3. However, in the next two sections, we will be presenting evidence against this sublinear hyperpolarizing mechanism.

A model for the nonlinear inhibition

We now present a division-like inhibitory mechanism that is based on a simple version of a shunting-inhibition model. This model will be developed, and its parameters will be fit to the experimental data, without the inclusion of conductance changes during the time course of the response. It nonetheless will prove consistent with the data presented here.

The synaptic model underlying our division-like mechanism appears in Fig. 4A. For the sake of generality, the model has both shunting and hyperpolarizing inhibitory components, and thus has division-like and subtraction-like properties. An almost pure hyperpolarizing mechanism corresponds to a large inhibitory battery (much more negative than the resting potential) and a small inhibitory conductance. The effect of this mechanism is to generate a negative current, which subtracts from the excitatory currents (Fig. 4B). On the other hand, a pure shunting-inhibition mechanism corresponds to a large conductance and a small battery (close to resting potential). Thus, the reduction in membrane resistance caused by shunting inhibition results in a decrease in the depolarization generated by the excitatory currents (Ohm's law). This changes the voltage–current slope, and accordingly, tends to divide the response *versus* excitatory function by a factor larger than one (Fig. 4B).

Now, we derive an equation for the response of the model of Figure 4A as a function of the contrasts of the first and second slits. The derivation of these equations assumes proportionality between the contrast of the first slit and the inhibitory conductance, and the contrast of the second slit and the excitatory conductance. (A Michaelis-Menten relationship may be used instead of a linear relationship for the dependence of the conductance on the contrast of the second slit without change in the functional form of the main equations). The resistance between the excitatory and inhibitory synapses is assumed to be large, and so the excitatory synapse can be approximated as a current source to the inhibitory conductance. Finally, the equations' derivation assumes a proportionality between membrane voltage at the output and the final spike count.

To derive this equation, observe that by Kirchhoff's and Ohm's laws the voltages at the different nodes of the model of Fig. 4A obey

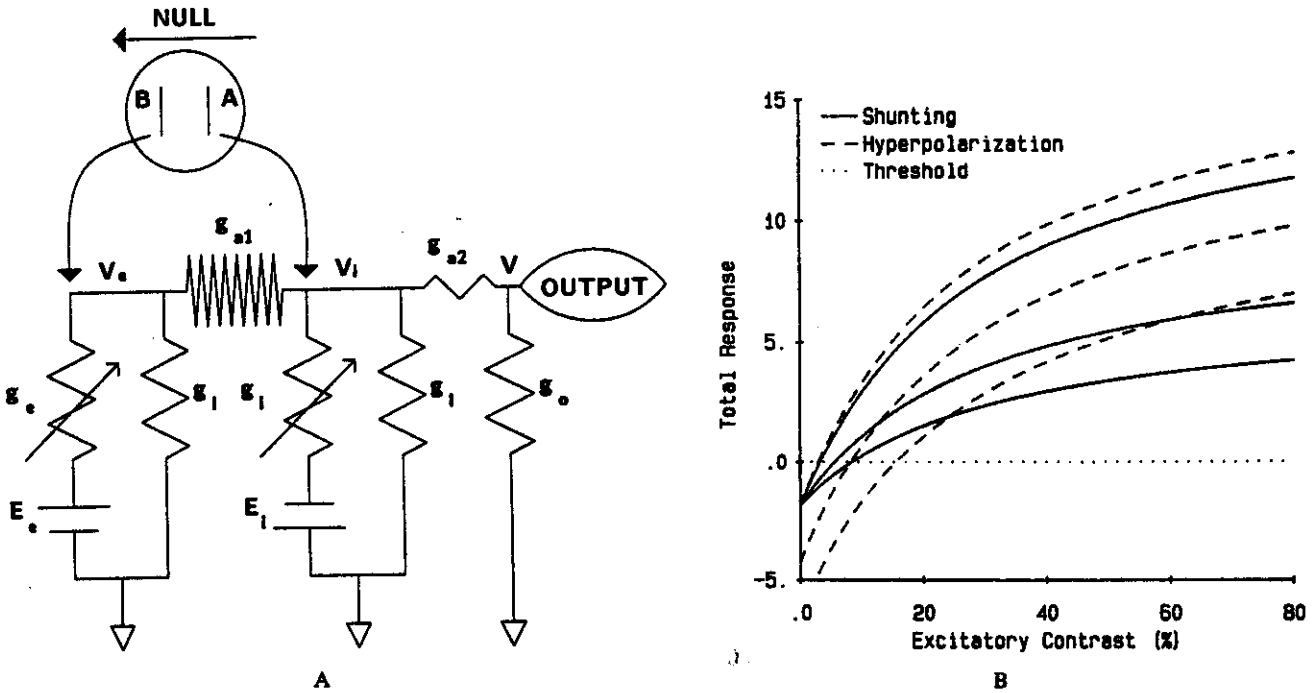

Fig. 4. A synaptic model for the inhibition involved in directional selectivity. A: The model's circuitry. Consider two slits of light, *A* and *B*, which appear in the receptive field as an apparent motion in the null direction. The model postulates that *B* generates excitation by the synaptic activation of a conductance, g_e, in a cell's dendritic tree. Also, we postulate that *A* counteracts this excitation through g_i, a conductance closer to the cell's output. This conductance inhibits the cell through its negative battery and through the shunting of the excitatory currents. If one assumes a large resistance (or small conductance g_{a1}) between the excitatory and inhibitory synaptic conductances and that they depend linearly on contrast, then eqn. (7) approximates this model. (Although this model is static, that is, neglect capacitors and synaptic time courses, it fits the data well.) B: The model's predictions. From eqn. (7), we plotted the predicted responses *versus* contrast functions of the second apparent-motion slit influenced by shunting or hyperpolarizing inhibition. In the shunting-inhibition case, the equation parameters were those of cell E380c3.1 in Table 1, except for $k_2 = 0$. In the hyperpolarization case, the parameters k_1 and a were maintained, but $k_2 = -50$ and $b = 0.005$. The effect of shunting inhibition is analogous to a division of the excitation function. This results in a marked decline in the vertical scale of the response-*versus*-contrast function, but little change in the takeoff from zero unless the threshold is very high. The effect of hyperpolarizing inhibition is to subtract a constant from the excitation, shifting the response-*versus*-contrast curve downward. The curve shape remains relatively constant, but the point at which it crosses threshold changes markedly.

$$g_e(E_e - V_e) - g_l V_e - g_{a1}(V_e - V_i) = 0, \quad (2a)$$

$$g_{a1}(V_e - V_i) - g_i(V_i - E_i) - g_l V_i - g_{a2}(V_i - V) = 0, \quad (2b)$$

$$g_{a2}(V_i - V) - g_o V = 0. \quad (2c)$$

These three equations are linear and their variables are V_e, V_i, and V. Thus, one can solve them for V to obtain

$$V = \frac{g_{a2}(g_{a1}g_e E_e + g_i(g_l + g_{a1} + g_e)E_i)}{(g_{a2} + g_o)((g_l + g_{a1} + g_e)(g_l + g_{a1} + g_{a2} + g_i) - g_{a1}^2) - g_{a2}^2(g_l + g_{a1} + g_e)} \quad (3)$$

The assumption that the resistance between the excitatory and inhibitory synapses is large simplifies eqn. (3) to

$$V = \frac{g_{a2}(g_{a1}g_e E_e + g_i(g_l + g_e)E_i)}{(g_l + g_e)((g_{a2} + g_o)(g_l + g_{a2} + g_i) - g_{a2}^2)} \quad (4)$$

This expression provides an evaluation of the total response R of the ganglion cell, because we assume that above the threshold T this response is proportional to V; that is,

$$R = \alpha V - T, \quad (5)$$

where α is a constant. We assume that the inhibitory and excitatory synaptic conductances are proportional to the contrast of the first slit c_i, and of the second slit c_e, respectively. If one chooses the coefficients of proportionality, a and b, to obey

$$ac_e = \left(\frac{1}{g_l}\right) g_e, \quad (6a)$$

$$bc_i = \left(\frac{g_{a2} + g_o}{g_l g_{a2} + g_l g_o + g_{a2} g_o}\right) g_i, \quad (6b)$$

then one can rewrite eqns. (4) and (5) as

$$R(c_e, c_i) = \frac{r(c_e) + k_2 bc_i}{1 + bc_i} - T, \quad (7a)$$

$$r(c_e) = k_1 \frac{ac_e}{1 + ac_e}, \quad (7b)$$

where

$$k_1 = \frac{\alpha g_{a1} g_{a2}}{g_1 g_{a2} + g_1 g_o + g_{a2} g_o} E_e, \tag{8a}$$

$$k_2 = \frac{\alpha g_{a2}}{g_{a2} + g_o} E_i. \tag{8b}$$

In what follows, we use eqn. (7) to fit the data. (Torre & Poggio, 1978 used a somewhat similar equation in their model of retinal directional selectivity.) The parameters k_1, k_2, a, and b are determined by the nonlinear fit procedure, while the parameter T is estimated by an independent method described in Table 1. The term r in the numerator of eqn. (7a) corresponds to the effect of a synaptic depolarizing current injected on dendrites far from the output. In turn, the term $k_2 bc_i$ corresponds to the effect of a hyperpolarizing current due to a more proximal synapse (Fig. 4B). This synapse's conductance, which is proportional to bc_i, divides the excitation (shunting inhibition, Fig. 4B). A Michaelis–Menten relationship describes the effect of the synaptic depolarizing current [eqn. (7b)]. Strictly speaking, T should depend on the slits' contrasts. It represents the number of extra spikes the response would have if there was no threshold after the output of Fig. 4A. Realistically, this number should increase as the response increases, since the output would spend more time above threshold. However, we approximate this number by a constant, because the output's threshold seems to be relatively low. To reach this conclusion, one must realize that in Fig. 2 the tail of the response tends to remain above zero even for high inhibition.

Equation (7a) helps explain why hyperpolarization is subtraction-like and shunting inhibition is division-like. Although the former appears in the numerator ($k_2 bc_i$) as a subtraction to excitation (because k_2 is negative), the latter appears in the denominator ($1 + bc_i$) dividing excitation.

Fit of nonlinear model

Figure 5 shows the data for the cell of Fig. 2 and the best least-squares fit of eqn. (7) as produced by a "quasi-Newton" convergence procedure. This procedure varied k_1, a, b, and k_2.

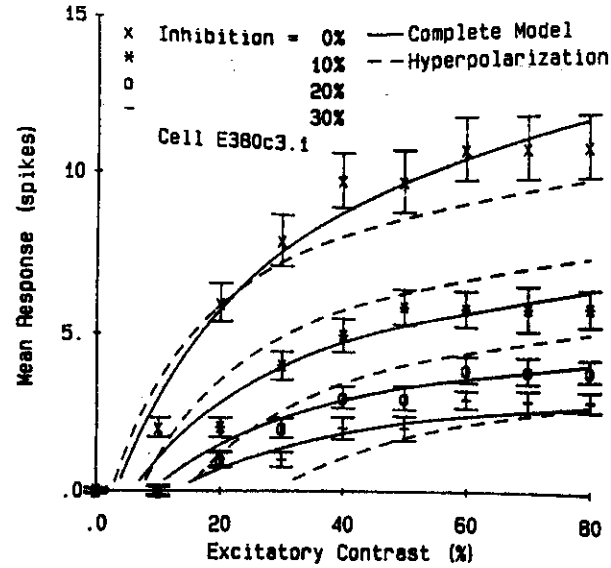

Fig. 5. Mean total-response data. These data, which pool both ON and OFF responses, appear against the contrast of the second slit (excitatory) and parametric on the contrasts of the first slit (inhibitory) for the same cell as in Fig. 2. The data are fitted with the full model of Fig. 4 (solid lines) and with only its hyperpolarizing term (dashed lines). Increasing inhibition caused a large decrease in the curves' vertical scale (high-gain inhibition) without large changes in the takeoff contrast. (Note that a threshold should cause some change in this takeoff contrast; Fig. 4B.) From the initial slope of the curve with no inhibition, this cell's threshold was estimated to be 1.9 spikes. The fit of the full model for this cell yielded an estimate for the hyperpolarizing term in eqn. (7), k_2, that was insignificantly different than zero (see Table 1). This fit was good, with a multiple correlation coefficient of 0.98. In contrast, the fit of the hyperpolarizing term alone was poor.

(The parameter T was estimated by an independent method, which is described in Table 1.) Because the procedure is sensitive to the initial guesses for the parameters, it was important to make good initial guesses. Our guesses corresponded to the behavior of eqn. (7) at special values of contrast, such as saturating and half-maximum contrasts.

Table 1. *Nonlinear estimates of the parameters of eqn. (7) by least-squares fit*

Cell	T (spikes)	k_1 (spikes)	a	k_2 (spikes)	b	r^2	$P<$
E374c4.1	4.9	32.5 ± 2.2	0.033 ± 0.006	0.6 ± 3.5	0.038 ± 0.016	0.98	0.0001
E375c2.1	3.7	33.4 ± 2.3	0.021 ± 0.003	−0.9 ± 1.5	0.039 ± 0.007	0.97	0.0001
E375c3.1	5.7	37.7 ± 2.6	0.028 ± 0.004	8.1 ± 1.2	0.063 ± 0.014	0.95	0.0002
E376c1.1	6.2	35.1 ± 1.8	0.039 ± 0.005	0.8 ± 2.3	0.063 ± 0.014	0.98	0.0001
E377c3.1	4.6	24.6 ± 2.3	0.035 ± 0.007	0.1 ± 11.9	0.057 ± 0.004	0.94	0.0139
E378c1.1	3.1	35.6 ± 4.3	0.013 ± 0.002	−6.6 ± 6.2	0.015 ± 0.006	0.98	0.0001
E379c2.1	3.0	23.6 ± 1.3	0.035 ± 0.005	2.6 ± 1.5	0.115 ± 0.033	0.98	0.0001
E380c3.1	1.9	18.5 ± 0.8	0.035 ± 0.003	−0.17 ± 0.59	0.061 ± 0.008	0.98	0.0001
E381c4.1	4.6	21.8 ± 0.9	0.042 ± 0.005	2.26 ± 0.36	0.060 ± 0.006	0.97	0.0001
E382c2.1	4.0	18.2 ± 2.0	0.045 ± 0.014	0.04 ± 2.0	0.059 ± 0.025	0.89	0.1314

The fits were good as indicated by the multiple correlation coefficient r^2. (For all cells, we calculated that the probabilities P that $r < 0.9$ was small—tested by the Fisher's z statistic (Dunn & Clark, 1987)). Physiological meaning of the parameters is given in the text. The parameter T was estimated by the intercept of the linear regression applied to the first two suprathreshold contrasts of the response-*versus*-contrast curve with the first-slit contrast set to zero. The parameters k_1, a, and b are relatively invariant across all ten cells and significantly positive. However, the parameter k_2, representing the hyperpolarization term, is not significantly different than zero, except for cells E375c3.1 and E381c4.1, where this parameter is slightly positive. This positivity corresponds to depolarization according to eqn. (7).

We now describe in detail how the initial parameter guesses for the fitting procedure were made. The maximal first-slit contrast (denoted $c_{i,max}$) and the maximal second-slit contrast (denoted $c_{e,max}$) were important in these guesses. From eqn. (7), one sees that the highest possible response is k_1 minus the threshold. Accordingly, the initial guess for k_1 (denoted $k_{1,i}$) was the sum of the estimated value of T and the data ordinate for $c_e = c_{e,max}$ and $c_i = 0$. Also, from eqn. (7), one can calculate when the response versus contrast curve reaches its half-maximum value. With no inhibition and discounting threshold, this happens when the contrast times a equals unity. Hence, the initial value of a was $1/c_e^*$, where c_e^* is the estimated second-slit contrast such that the linearly interpolated value of the response with $c_i = 0$ is $k_{1,i}/2 - T$. To make initial guesses for k_2 (denoted $k_{2,i}$) and for b (denoted b_i), we used the data ordinate (denoted R^*) for $c_e = c_{e,max}$ and $c_i = c_{i,max}$. There were two pairs of initial guesses for $k_{2,i}$ and b_i: In the first pair, $k_{2,i} = 0$ and b_i satisfied $R^* = k_{1,i}/(1 + b_i c_{i,max}) - T$ so that only shunting inhibition mattered. In the second pair, $b_i c_{i,max} = 0.1$ and $k_{2,i}$ satisfied $R^* = k_{i,1} + k_{2,i} b_i c_{i,max}$ so that shunting inhibition was practically irrelevant and inhibition was due to hyperpolarization. For all cells, these two pairs of initial guesses yielded identical results for the final output of the fitting procedure. This strongly indicates that the best fit was found.

The model provided a statistically good fit to the data (details below). (Also, the statistical significance was relatively independent of the assumption that the resistance between the excitatory and inhibitory processes was large, not reported here.)

In virtually every characteristic, the effect of the first slit is consistent with shunting, not hyperpolarizing, inhibition. In the model fit, the parameter k_2, the maximal contribution of the hyperpolarizing term, is -0.17 ± 0.60 (S.E.) spikes, which is not significantly different than zero. On the other hand, the parameter b, which controls shunting inhibition, is significantly positive; $b = 0.061 \pm 0.008$. Thus, according to the model's interpretation, the membrane resistance decreases by a factor of $(1 + bc_i) = 2.8$ from the non-inhibition situation to the situation of 30% contrast in the first slit. (This result suggests that the inhibition was high gain.) This result is emphasized by the contrasting failure of the hyperpolarizing term alone to fit the data well (also shown in Fig. 5). To demonstrate this failure, we computed the best fit of eqn. (7) limited by significant contribution only from the hyperpolarizing term. In this fit, the value of b was forced to satisfy $bc_{i,max} < 0.1$. (The initial guesses of k_1 and a for the fitting procedure were as above, and the initial guess of k_2 satisfied $R^* = k_{i,1} + k_{2,i} b_i c_{i,max} - T$.)

Table 1 shows the parameters of the best fit of the model for all ten cells including the multiple correlation coefficients (the total goodness-of-fit parameters). All ten cells were well-fitted by this model (tested by the Fisher's z statistic—Dunn & Clark, 1987) with consistent estimates of all of the essential parameters, except for the linear hyperpolarizing term k_2. This term was never significantly negative, which according to eqn. (7) appears to suggest that hyperpolarizing inhibition does not contribute to directional selectivity. However, the b parameter was always significantly positive, which favors a shunting-inhibition model. The parameter k_2 was significantly nonzero in only two cases: cells E375c3.1 and E381c4.1. In both cases, this parameter was small but positive. This positivity corresponds to a depolarization [see eqn. (7)] and could conceivably produce a facilitation of the responses to some stimuli (Torre & Poggio, 1978), which has been observed (Barlow & Levick, 1965; Grzywacz & Amthor, 1989*a*).

Discussion

We have shown evidence that linear inhibition does not mediate retinal directional selectivity, but that a division-like, possibly shunting, inhibition may. Shunting inhibition would have the advantage that its effect could be relatively confined to specific dendritic tree branches (Torre & Poggio, 1978). This would allow local computations by which *single* cells could generate receptive fields with multiple directionally selective regions, as observed by Barlow and Levick (1965). However, these local computations do not imply that the shunting synapses must be located far from the output. There are shunting-inhibition models, consistent with Barlow and Levick's observations, in which shunting synapses contact the entire dendritic tree (Koch et al., 1982; Grzywacz & Amthor, 1989*b*).

Because shunting inhibition is consistent with Fig. 5, we wondered whether this type of inhibition may account for the linearity of Fig. 3, its zero intercept, and its near unity slope. To analyze this problem, one needs to compute the time course of the inhibitory strength [eqn. (1)] under an assumption of shunting inhibition. The simplest of such assumptions postulates that $R_c(t) = R_0(t)/(1 + bc)$, where b has the same interpretation as in eqn. (7). By substituting this into eqn. (1), one obtains

$$S_c(t) = \left(\frac{bc}{1 + bc}\right) R_0(t). \tag{9}$$

Now consider the plot of $S_{c_2}(t)$ as a function of $S_{c_1}(t)$. Because $R_0(t)$ is common to all contrasts, this plot should be a straight line with zero intercept. From eqn. (10), the slope of this line can be calculated to be $(c_2/c_1)((1 + bc_1)/(1 + bc_2))$. This slope is smaller than c_2/c_1, which was the slope predicted by linear inhibition [see discussion after eqn. (1)]. Also, this slope decreases with b, approaching unity as b goes to infinity.

Thus, shunting inhibition alone may lead to the linear features observed in Fig. 3. However, from the value of b given in Table 1, we calculate that the slope in Fig. 3 should have been about 1.45, which is higher than observed. Why is there a discrepancy between predicted and observed slopes? The large slope calculated from Table 1 indicates a weaker average inhibition for the total response than for the portions of response used in Fig. 3. These portions tended to be near the maxima of the histograms to avoid threshold effects (see Methods). Thus, this analysis suggests that inhibition is stronger near the maximum of the response than during the response's late tail. Direct inspection of the histograms plotted in Fig. 2 provides support for this suggestion. The inhibition's late weakening is probably not due to a decay of the effects of the first slit. We reached this conclusion because other two-slit experiments which varied inter-slit delay showed that the inhibitory strength varies little with delay for delays up to 2 s (Amthor & Grzywacz, 1988). Rather, we speculate that the late weakening of inhibition is due to a process activated by the response to the second slit. Such a process might, for example, be mediated by the late activation of voltage-dependent channels, which would make the cells insensitive to modulations of their inputs' amplitude (Madison & Nicoll, 1982). This mechanism might thus lead to a late desensitization of inhibition.

Finally, one may ask whether a linear inhibition might mediate directional selectivity, but is "spoiled" by a later nonlinearity leading to our results. Qualitatively, the answer to this question is positive: consider, for example, that this nonlinearity is supralinear, that is, the first derivative of the input–output relationship increases with the magnitude of the input. (Such a nonlinearity could arise from a cooperative synaptic transmission [Dodge & Rahamimoff, 1967; Smith et al., 1985] or from the transition from primary to secondary range [Kernell, 1970; Schwindt & Crill, 1982] in the firing of ganglion cells.) In this case, the responses without inhibition are emphasized such that relatively, inhibition brings the responses closer to zero, practically irrespectively of the first slit's contrast. Thus, the inhibitory strength [eqn. (1)] might be relatively independent of contrast for intermediate and high contrasts. This would lead to the linear behavior, zero intercept, and near-unity slope observed in Fig. 3. Furthermore, for every second-slit contrast, the slope of the total response versus contrast curve may decrease with inhibitory strength as in Fig. 5. To see this, rewrite eqn. (7) without shunting inhibition, with $T = 0$, and with a supralinearity given by the function $S(x)$, such that $S''(x) > 0$, where a prime stands for derivative. This means that we rewrite eqn. (7) as $R(c_e, c_i) = S(r(c_e) + k_2 b c_i)$. The partial derivative of the response, $R(c_e, c_i)$, by c_e is $S'(r(c_e) + k_2 b c_i) r'(c_e)$, and therefore, this derivative decreases with the strength of inhibition, because $S''(x) > 0$. Thus, the possibility of a linear inhibition followed by a supralinearity cannot be ruled out. (A mechanism related, but not equivalent, to supralinearity is a high threshold. We rule out such a mechanism based on a series of experiments with low contrast sinusoidal gratings [Grzywacz et al., 1990]).

In conclusion, although a linear inhibitory mechanism followed by a nonlinearity remains possible, the *overall* behavior of null-direction inhibition is nonlinear and division-like. Unraveling the biophysical basis of this behavior will require additional experiments.

Acknowledgments

We thank Lyle Borg-Graham and Tomaso Poggio for helpful discussions during the realization of this project. Also, we thank Richard Andersen, Horace Barlow, Lyle Borg-Graham, John Dowling, and Tomaso Poggio for critically reading early versions of this manuscript. F. R. Amthor was supported by grants from the National Institute of Health (EY05070) and the Sloan Foundation. N. M. Grzywacz was supported by the Grant BNS-8809528 from the National Science Foundation, by the Sloan Foundation, by a grant to Tomaso Poggio, Ellen Hildreth, and Peter Schiller from the Office of Naval Research, Cognitive and Neural Systems Division, and by the Grant IRI-8719394 to Tomaso Poggio, Ellen Hildreth, and Edward Adelson from the National Science Foundation.

References

Adelson, E.H. & Bergen, J.R. (1985). Spatio-temporal energy models for the perception of motion. *Journal of the Optical Society of America A* **2**, 284–299.

Albrecht, D.G. & De Valois, R.L. (1981). Striate cortex responses to periodic patterns with and without the fundamental harmonics. *Journal of Physiology* **319**, 497–514.

Ames, A.A., III & Hastings, A.B. (1956). Studies on water and electrolytes in nervous tissue. *Journal of Neurophysiology* **19**, 201–212.

Amthor, F.R. & Grzywacz, N.M. (1988). The time course of inhibition and the velocity independence of direction selectivity in the rabbit retina. *Investigative Ophthalmology and Visual Science* **29**, 225.

Amthor, F.R., Oyster, C.W. & Takahashi, E.S. (1984). Morphology of ON-OFF direction-selective ganglion cells in the rabbit retina. *Brain Research* **298**, 187–190.

Amthor, F.R., Takahashi, E.S. & Oyster, C.W. (1989). Morphologies of rabbit retinal ganglion cells with complex receptive fields. *Journal of Comparative Neurology* **280**, 97–121.

Ariel, M. & Adolph, A.R. (1985). Neurotransmitter inputs to directionally sensitive turtle retinal ganglion cells. *Journal of Neurophysiology* **54**, 1123–1143.

Ariel, M. & Daw, N.W. (1982). Pharmacological analysis of directionally sensitive rabbit retinal ganglion cells. *Journal of Physiology* **324**, 161–185.

Barlow, H.B. & Levick, W.R. (1965). The mechanism of directionally selective units in rabbit's retina. *Journal of Physiology* **178**, 477–504.

Caldwell, J.H., Daw, N.W. & Wyatt, H.J. (1978). Effects of picrotoxin and stychnine on rabbit retinal ganglion cells: lateral interactions for cells with more complex receptive fields. *Journal of Physiology* **276**, 277–298.

Coombs, J.S., Eccles, J.C. & Fatt, P. (1955). The inhibitory suppression of reflex discharges from motoneurones. *Journal of Physiology* **130**, 396–413.

Dacheux, R.F., Delmelle, M., Miller, R.F. & Noell, W.K. (1973). Isolated rabbit retina preparation suitable for intracellular and extracellular analysis. *Federation Proceedings* **32**, 327.

DeVoe, R.D., Carras, P.L., Criswell, M.H. & Guy, R.G. (1989). Not by ganglion cells alone: Directional selectivity is widespread in identified cells of the turtle retina. In *Neurobiology of the Inner Retina*, ed. Weiler, R. & Osborne, N.N., pp. 235–246. Berlin, F.R.G.: Springer-Verlag.

Dodge, F.A. & Rahamimoff, R. (1967). Cooperative action of calcium ions in transmitter release at the neuromuscular junction. *Journal of Physiology* **193**, 419–432.

Dowling, J.E. (1987). *The Retina: An Approachable Part of the Brain*. Cambridge, Massachusetts: Harvard University Press.

Dunn, O.J. & Clark, V.A. (1987). *Applied Statistics: Analysis of Variance and Regression*. New York: John Wiley.

Grzywacz, N.M. & Amthor, F.R. (1988). What are the directionally selective subunits of rabbit retinal ganglion cells? *Society for Neuroscience Abstracts* **14**, 603.

Grzywacz, N.M. & Amthor, F.R. (1989*a*). Facilitation in ON-OFF directionally selective ganglion cells of the rabbit retina. *Society for Neuroscience Abstracts* **15**, 969.

Grzywacz, N.M. & Amthor, F.R. (1989*b*). A computationally robust anatomical model for retinal directional selectivity. In *Advances in Neural Information Processing Systems Vol. 1*, ed. Touretzky, D.S., pp. 477–484. Palo Alto, California: Morgan Kaufman Publishers.

Grzywacz, N.M., Amthor, F.R. & Mistler, L.A. (1990). Applicability of quadratic and threshold models to motion discrimination in the rabbit retina. *Biological Cybernetics* **64**, 41–49.

Grzywacz, N.M. & Koch, C. (1987). Functional properties of models for direction selectivity in the retina. *Synapse* **1**, 417–434.

Grzywacz, N.M. & Yuille, A.L. (1990). A model for the estimate of local image velocity by cells in the visual cortex. *Proceedings of the Royal Society B* (London) **239**, 129–161.

Heeger, D.J. (1987). A model for the extraction of image flow. *Journal of the Optical Society of America A* **4**, 1455–1471.

Jack, J.J.B., Noble, D. & Tsien, R.W. (1975). *Electric Current Flow in Excitable Cells*. Hong Kong: Clarendon Press.

Kandel, E.R. & Schwartz, J.H. (1985). *Principles of Neural Science*. New York: Elsevier.

Kernell, D. (1970). Cell properties of importance for the transfer of signals in nervous pathways. In *Excitatory Synaptic Mechanisms* ed. Andersen, P.O. & Jansen, J., pp. 269–273. Oslo, Norway: Universitetsforlag.

Koch, C., Poggio, T. & Torre, V. (1982). Retinal ganglion cells: a functional interpretation of dendritic morphology. *Philosophical Transactions of the Royal Society B* **298**, 227–264.

Madison, D.V. & Nicoll, R.A. (1982). Noradrenaline blocks accommodation of pyramidal cell discharge in the hippocampus. *Nature* **299**, 636–638.

Marchiafava, P.L. (1979). The responses of retinal ganglion cells to stationary and moving visual stimuli. *Vision Research* **19**, 1203–1211.

Masland, R.H., Mills, W. & Cassidy, C. (1984). The functions of acetylcholine in the rabbit retina. *Proceedings of the Royal Society B* (London) **223**, 121–139.

MILLER, R.F. (1979). The neuronal basis of ganglion-cell receptive-field organization and the physiology of amacrine cells. In *The Neurosciences Fourth Study Program*, ed. SCHMITT, F.O. & WORDEN, F.G., pp. 227–245. Cambridge, Massachusetts: MIT Press.

POGGIO, T. & REICHARDT, W.E. (1973). Considerations on models of movement detection. *Kybernetik* **13**, 223–227.

RALL, W. (1964). Theoretical significance of dendritic trees for neuronal input–output relations. In *Neural Theory and Modelling*, ed. REISS, R.F., pp. 73–79. Stanford, California: Stanford University Press.

SCHWINDT, P.C. & CRILL, W.E. (1982). Factors influencing motoneuron rhythmic firing: results from a voltage-clamp study. *Journal of Neurophysiology* **48**, 875–890.

SHAPLEY, R.M. & VICTOR, J.D. (1980). The effect of contrast on the nonlinear response of the Y cell. *Journal of Physiology* **302**, 535–547.

SMITH, S.J., AUGUSTINE, G.J. & CHARLTON, M.P. (1985). Transmission at voltage-clamped giant synapse of the squid: evidence for cooperativity of presynaptic calcium action. *Proceedings of the National Academy of Sciences of the U.S.A.* **82**, 622–625.

STEPHENS, M.A. (1987). Regression tests of fit. In *Goodness-of-Fit, Colloquia Mathematica Societatis János Bolyai, Vol. 45*, ed. RÉVÉSZ, P., SARKADI, K. & SEN, P.K., pp. 541–557. Amsterdam: North-Holland Publishing Company.

TORRE, V. & POGGIO, T. (1978). A synaptic mechanism possibly underlying directional selectivity to motion. *Proceedings of the Royal Society B* (London) **202**, 409–416.

VANEY, D.I. & YOUNG, H.M. (1988). GABA-like immunoreactivity in cholinergic amacrine cells of the rabbit retina. *Brain Research* **438**, 369–373.

VICTOR, J.D. (1987). The dynamics of the cat retina X cell centre. *Journal of Physiology* (*London*) **386**, 219–246.

VICTOR, J.D. (1988). The dynamics of the cat retina Y cell subunit. *Journal of Physiology* (*London*) **405**, 289–320.

WATANABE, S.-I. & MURAKAMI, M. (1984). Synaptic mechanisms of directional selectivity in ganglion cells of frog retina as revealed by intracellular recordings. *Japanese Journal of Physiology* **34**, 497–511.

WYATT, H.J. & DAW, N.W. (1975). Directionally sensitive ganglion cells in the rabbit retina: specificity for stimulus direction, size, and speed. *Journal of Neurophysiology* **38**, 613–626.